

High transmission contrast for single resonator based all-optical diodes with pump-assisting

Xu-Sheng Lin^{1*}, Jun-Hu Yan¹, Li-Jun Wu², and Sheng Lan²

¹*School of Electronic and Information Engineering, Guangdong Polytechnic Normal University, Guangzhou 510665, China*

²*Laboratory of Photonic Information Technology, School for Information and Optoelectronic Science and Engineering, South China Normal University, Guangzhou 510006, China*

*Corresponding author: xslin64@yahoo.cn

Abstract: We present a detailed analysis of realizing the unidirectional transmission by using the bistability of a nonlinear optical resonator. We show that the transmission contrast can be enhanced by an order of magnitude if the upper branch of hysteresis loop is explored with pump-assisting. It provides all-optical diodes with simple configuration and high transmission contrast.

©2008 Optical Society of America

OCIS codes: (190.1450) Bistability; (230.3240) Isolators; (230.5298) Photonic crystals.

References and links

1. H. Kuwahara, "Optical isolator for semiconductor lasers," *Appl. Opt.* **19**, 319-324(1980).
2. M. Levy, R. M. Osgood, Jr., H. Hegde, F. J. Cadieu, R. Wolfe, and V. J. Fratello, "Integrated optical isolators with sputter-deposited thin-film magnets," *IEEE Photon. Technol. Lett.* **8**, 903-905(1996).
3. Z. Yu, Z. Wang, and S. Fan, "One-way total reflection with one-dimensional magneto-optical photonic crystals," *Appl. Phys. Lett.* **90**, 121133(2007).
4. M. Scalora, J. P. Dowling, C. M. Bowden, and M. J. Bloemer, "The photonic band edge optical diode," *J. Appl. Phys.* **76**, 2023-2026(1994).
5. K. Gallo and G. Assanto, "All-optical diode in a periodically poled lithium niobate waveguide," *Appl. Phys. Lett.* **79**, 314-316 (2001).
6. S. F. Mingaleev and Yuri S. Kivshar, "Nonlinear transmission and light localization in photonic crystal waveguides," *J. Opt. Soc. Am. B* **19**, 2241-2249 (2002).
7. S. Pereira, P. Chak, J. E. Sipe, L. Tkeshelashvili, and K. Busch, "All-optical diode in an asymmetrically apodized Kerr nonlinear microresonator system," *Photonics Nanostruct. Fundam. Appl.* **2**, 181-190 (2004).
8. M. W. Feise, I. V. Shadrivov, and Yuri S. Kivshar, "Bistable diode action in left-handed periodic structures," *Phys. Rev. E* **71**, 037602 (2005).
9. J. Hwang, M. H. Song, B. Park, S. Nishimura, T. Toyooka, J. W. Wu, Y. Takanishi, K. Ishikawa, and H. Takezoe, "Electro-tunable optical diode based on photonic bandgap liquid-crystal heterojunctions," *Nature Mater.* **4**, 383-387 (2005).
10. X. S. Lin and S. Lan, "Unidirectional transmission in asymmetrically confined photonic crystal defects with Kerr nonlinearity," *Chin. Phys. Lett.* **22**, 2847-2850 (2005).
11. Andrey E. Miroshnichenko, Igor Pinkevych, and Yuri S. Kivshar, "Tunable all-optical switching in periodic structures with liquid-crystal defects," *Opt. Express* **14**, 2839-2844(2006).
12. X. S. Lin, W. Q. Wu, H. Zhou, K. F. Zhou, and S. Lan, "Enhancement of unidirectional transmission through the coupling of nonlinear photonic crystal defects," *Opt. Express* **14**, 2429-2439(2006).
13. N. S. Zhao, H. Zhou, Q. Guo, W. Hu, X. B. Yang, S. Lan, and X. S. Lin, "Design of highly efficient optical diodes based on the dynamics of nonlinear photonic crystal molecules," *J. Opt. Soc. Am. B*, **23**, 2434-2440(2006).
14. A. Alberucci and G. Assanto, "All-optical isolation by directional coupling," *Opt. Lett.* **33**, 1641-1643 (2008).
15. E. Centeno and D. Felbacq, "Optical bistability in finite-size nonlinear bidimensional photonic crystals doped by a microcavity," *Phys. Rev. B* **62**, R7683-R7686 (2000).
16. E. Lidorikis and C. M. Soukoulis, "Pulse-driven switching in one-dimensional nonlinear photonic band gap materials: a numerical study," *Phys. Rev. E* **61**, 5825-5829 (2000).
17. M. Soljačić, M. Ibanescu, S. G. Johnson, Y. Fink, and J. D. Joannopoulos, "Optimal bistable switching in nonlinear photonic crystals," *Phys. Rev. E* **66**, 055601(R) (2002).
18. M. F. Yanik, S. Fan, and M. Soljačić, "High-contrast all-optical bistable switching in photonic crystal microcavities," *Appl. Phys. Lett.* **83**, 2739-2741(2003).

1. Introduction

All-optical diodes or isolators have great potential applications in high-density integrated optical circuits. As the traditional devices based on the Faraday rotation effect or other magneto-optical phenomena need external magnetic fields [1-3], some researchers turn to develop the all-optical diodes by using the nonlinear optical effects [4-14]. The bistability, which can be achieved by using a photonic crystal (PC) resonator with Kerr nonlinearity [15-18], attracts considerable attention [6, 8, 10-13].

To date, all the PC-based all-optical diodes belong to the self-inducing type, i.e., the unidirectional transmission is accomplished by the input signal without involving any external pumps. Such operations are simple, but there is a demerit of low transmission contrast [6, 8, 10]. To some extent, this can be solved by adopting structures that contain two or more coupled resonators, but the couplings among the resonators and the resonant frequencies have to be modulated carefully [12, 13]. Also, in practice, the signal would suffer more loss due to the longer stay in the devices. Therefore, achieving high transmission contrast by employing single resonator structures is very desirable. In this paper, we give a possible solution to the problem by exploring the bistability of an asymmetrically confined PC resonator with pump-assisting. It shows theoretically and numerically that the transmission contrast can be greatly enhanced.

2. Bistability of PC resonators with Kerr nonlinearity

As had been studied by Soljačić *et al*, the bistability transmission of a PC resonator with Kerr nonlinearity can be described by using the first-order perturbation theory [17]

$$T = \frac{P_{\text{out}}}{P_{\text{in}}} = \frac{1}{1 + (P_{\text{out}}/P_0 - \delta)^2}, \quad (1)$$

where P_{out} and P_{in} are the steady output and input powers, δ is the detuning of the input frequency ω to the resonant frequency ω_0 , i.e., $\delta = (\omega_0 - \omega)/\gamma$ with γ the width of the PC resonance, P_0 is the characteristic power reflecting the nonlinear feedback and power confinement of the resonator [17]. For the asymmetrically confined resonator, P_0 depends on the launch direction because different coupling strength between the input waveguide and the resonator brings different nonlinear enhancement inside the resonator [10, 12]. Thus, according to Eq. (1), the hysteresis loops corresponding to two launch directions are not the same. For some input powers, very large discrepancy between the transmissions of the two launch directions exists. Based on the phenomenon, the asymmetrically confined PC resonator can work as an all-optical diode.

To explain the working mechanism, consider a nonlinear PC resonator that connects two I/O waveguides at its left and right sides. Suppose the characteristic powers corresponding to the rightward and leftward launches, denoted as P_{0R} and P_{0L} , meet $P_{0L} = 1.5P_{0R}$, and the input frequency detuning $\delta = 4.0$, then, we can plot the hysteresis loops for the two launch directions by using Eq. (1). They are shown in Fig. 1 by the red (rightward launch) and blue (leftward launch) curves, the dashed are the unstable states that cannot be realized in practice. Furthermore, four vertical arrows are presented to indicate the critical transitions between the lower and upper transmission states. We see that bistability transmission appears at different ranges of input power, with about $(4\sim 11)P_{0R}$ for the rightward launch and about $(6\sim 16)P_{0R}$ for the leftward launch.

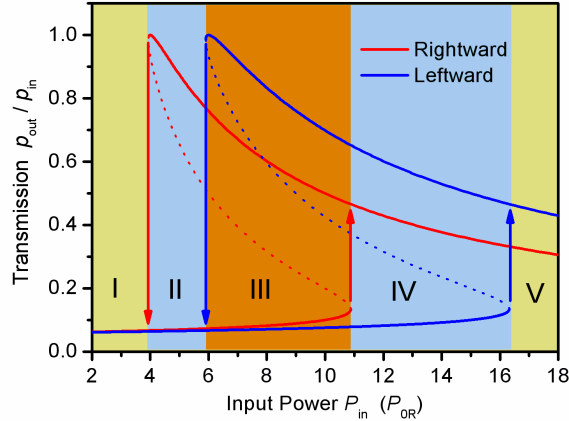


Fig. 1. Theoretical hysteresis loops of the asymmetrically confined PC resonator that correspond to the rightward (red) and leftward (blue) launches under the conditions of $P_{0L}=1.5P_{0R}$ and $\delta = 4.0$. Obviously unidirectional transmission occurs in Part II and Part IV.

For the sake of convenience, we divide the range of input power into five parts, as shown in Fig. 1. In Part I and V, the leftward and rightward transmissions are at the lower branches (Part I) or the upper branches (Part V) at the same time, so it is not suitable for unidirectional transmissions. In Part IV, the input powers are able to maintain the rightward transmission at the upper branch, but they are still not strong enough to boost the leftward transmission to the upper branch. In this way, the resonator behaves unidirectional transmission. We call it self-inducing unidirectional transmission as no external pump pulse involves. It is the area at which the ordinary all-optical diode works [6, 8, 10-13]. Intuitively, the transmission contrast ratio, defined as the ratio of transmissions from the rightward and leftward launches for the same input, is not very large. In Part III, every transmission has two stable states, but it is difficult to make the rightward and leftward transmissions stand at different branch, so unidirectional transmission cannot be achieved easily.

Now we focus on Part II where the leftward transmission stays only at the lower branch. It is clear that if we manage to make the rightward transmission rest on the upper branch, the transmission contrast can be very high, even much higher than that in Part IV. Actually, by using Eq. (1), the maximum contrast ratio C_{\max} can be estimated readily as $\sim(1 + \delta^2)$, which shows no upper limit because δ can be set at any values theoretically. As for the diodes work in Part IV, there is an upper limit of $C_{\max} < 9$ [10]. Of course, to realize the unidirectional transmission in Part II, one needs an additional pump pulse to excite the resonator into the higher transmission state. By doing so, it can rest on the upper branch even when the pump pulse is over [16, 17]. For the leftward launch, the stable transmissions are at the lower branch whether we superpose the pump pulse or not, as no upper branch for the leftward launch exists in Part II. Therefore, we are sure that high transmission contrasts can be achieved in Part II by pump-assisting. Apparently, it belongs to the logic operation that requires input, output, and control signals.

3. Nonlinear FDTD simulations

To support the above analysis, we carry out simulations on the simple model shown in Fig. 2 by using the nonlinear finite-difference time-domain (FDTD) technique [19]. It is a square lattice of GaAs rods embedded in air. The refractive index and the nonlinear coefficient are 3.40 and $1.5 \times 10^{-5} \mu\text{m}^2/\text{W}$, respectively. The radius of the normal rods is chosen to be $0.30a$ with the lattice constant a equal to $0.60 \mu\text{m}$. A defect resonator is introduced by reducing the radius of the centre rod to $0.15a$. To make the resonator asymmetrically confined, the radii of the two dielectric rods located at the left side of the defect rod are changed to $0.25a$. Two PC waveguides serving as I/O ports are created by removing three lines of the dielectric rods. For

the transverse magnetic modes whose electric field parallels to the rods, it can be calculated that the band gap ranges from $0.233(2\pi c/a)$ to $0.299(2\pi c/a)$, where c is the speed of light in vacuum. The resonant frequency ω_0 and the linewidth γ of the resonator are $0.257(2\pi c/a)$ and $0.306 \times 10^{-3}(2\pi c/a)$, respectively.

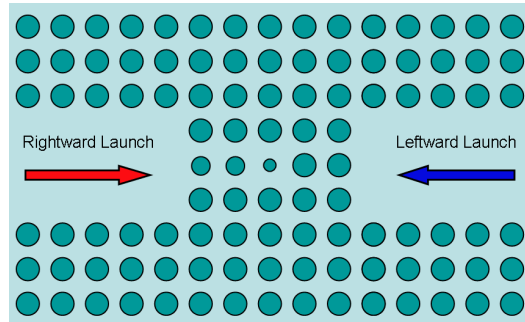


Fig. 2. Schematic PC resonator that contains a defect rod at the centre with a $0.15a$ radius, where a is the lattice constant. The radii of the normal rods are $0.30a$ while the radii of the two rods located at the left side of the defect rod are changed to $0.25a$.

To start with, continue wave (CW) of a given frequency detuning, say $\delta = 4.0$, with Gaussian spatial shape is launched from the left port into the resonator, different stable output powers can be measured by a monitor set at the right port while increasing the input power. In this way, we obtain the lower branch of hysteresis loop for the rightward launch case, as the red empty circles shown in Fig. 3. The transmission jumps to the upper branch when the input power is about $12.3 \text{ W}/\mu\text{m}$, and it gets a little smaller when the input power increases further. To obtain the upper branch of the loop, the CW input is superposed with a high peak-power Gaussian pulse, as had been suggested in Refs. [16] and [17]. Stable output powers can be measured when the pulse is over. The resulting transmissions are presented as red solid circles in the same figure. It drops to the lower branch when the input power of CW is about $8.7 \text{ W}/\mu\text{m}$. So, for the rightward launch case, the transmission can stick to the upper branch by pump-assisting when the input power is among $(8.7\sim 12.3) \text{ W}/\mu\text{m}$. By similar simulations, we can get the hysteresis loop of the leftward launch case, as shown in Fig. 3 by the blue empty circles (CW only) and solid circles (CW superposed with Gaussian pulse). We see that the leftward transmissions stick to the upper branch by pump-assisting when the input power is among $(9.9\sim 13.8) \text{ W}/\mu\text{m}$.

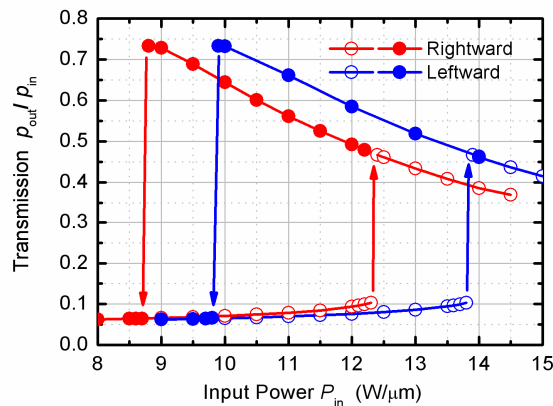


Fig. 3. Simulational hysteresis loops of the asymmetrically confined PC resonator that correspond to the rightward (red circles) and leftward (blue circles) launches when the input frequency detuning is 4.0

Based on the results in Fig. 3, we find that (a) self-inducing unidirectional transmission occurs when the input power is among (12.3~13.8) W/ μm , with a maximum contrast ratio of about 5 and a maximum positive transmission of about 0.46. No external pump is needed; (b) pump-assisting unidirectional transmission occurs when the input power is among (8.7~9.9) W/ μm , with a maximum contrast ratio of about 12 and a maximum positive transmission of about 0.74. It needs a pump pulse.

In order to fully compare the two types of operation, we present in Fig. 4(a) the maximum contrast ratio C_{max} and Fig. 4(b) the maximum positive transmission T_p for several frequency detunings δ , using the nonlinear FDTD simulation results. In Fig. 4(a), it is found that with pump-assisting C_{max} can be enhanced by an order of magnitude when compared with the self-inducing case. For the pump-assisting case, C_{max} increases with δ with a tendency close to $(1 + \delta^2)$. It reaches 36 when δ is 7. In contrast, C_{max} in the self-inducing case has an upper limit of about 7, very similar to the results in Ref. [10] where a PC resonator created in a slab waveguide was employed. As for the maximum positive transmission T_p , which is also an important factor for practical operations, Fig. 4(b) shows that it decreases with δ for both cases. Nevertheless, when δ changes from 2.5 to 7.0, T_p reduces only from 0.80 to 0.55 for the pump-assisting case, while it drops significantly from 0.80 to 0.18 for the self-inducing case. Therefore, the pump-assisting diode performs much better than the self-inducing one as δ increases.

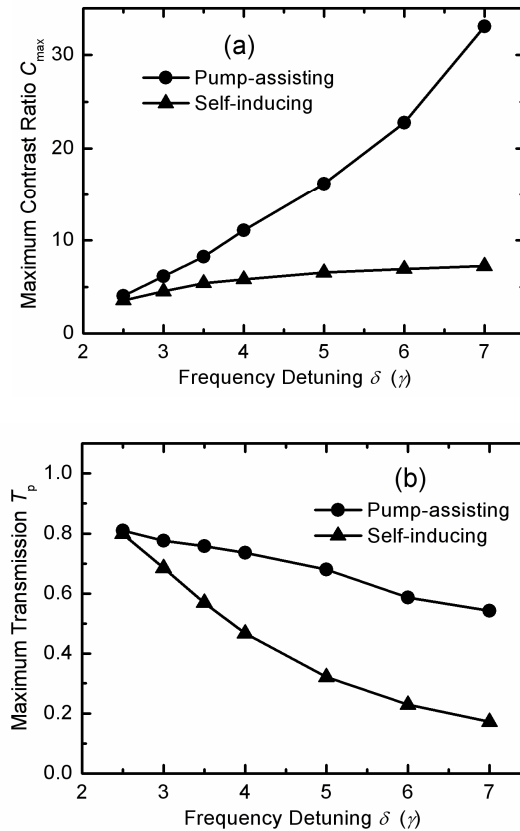


Fig. 4. Comparison between the pump-assisting and self-inducing operations (a) the maximum transmission contrast ratio; (b) the maximum positive transmission for CWs with different frequency detuning.

4. Conclusion

We have discussed how to achieve high transmission contrast for the optical diodes that base on the single PC resonator structures. With the assistance of pump pulses, we find that the problem can be solved by exploring the upper branch of the transmission loops. Our analyses are supported by the nonlinear FDTD simulation results.

Acknowledgments

The authors acknowledge the financial support from the National Natural Science Foundation of China (Grant Nos. 60778032 and 10674051).